

# High resolution WRF climatic simulations for the Iberian Peninsula: Model validation

Martinho Marta-Almeida<sup>a</sup>, João C. Teixeira<sup>b</sup>, Maria João Carvalho<sup>b</sup>, Paulo Melo-Gonçalves<sup>b</sup>,  
Alfredo M. Rocha<sup>b</sup>

<sup>a</sup>*Departamento de Ambiente e Ordenamento, CESAM-Universidade de Aveiro, Campus de Santiago 3810-193 Aveiro, Portugal*

<sup>b</sup>*Departamento de Física, CESAM-Universidade de Aveiro, Campus de Santiago 3810-193 Aveiro, Portugal*

---

## Abstract

A high resolution atmospheric modelling study was done for a 20-year recent historical period. The dynamic downscaling approach adopted used the Max Planck Institute Earth System Model (MPI-ESM) to drive the WRF running in climate mode. Three online nested domains were used covering part of the North Atlantic and Europe, with a resolution 81 km, and reaching 9 km in the innermost domain which covers the Iberian Peninsula.

For validation purposes, an additional configuration forced by the ERA-Interim reanalysis was also run. Validation was based on comparison of probability distributions between model results and observational datasets of near surface temperature and precipitation. The comparison was based on daily climatologies, spatially averaged inside subdomains obtained with cluster analysis of the observations, for each of the four seasons. The validation of the historic simulation was done in order to assess if the climate mode can be used to drive the regional WRF configuration, to estimate climate change projections for future time periods.

Considering the difficulty to simulate extremes in long term simulations, the results showed a comfortable comparison of both models (forced by climate model and reanalysis results) with observations. This provides us confidence on the continuity of using MPI-ESM to perform climate simulations of the future.

*Keywords:* Dynamical Downscaling, Climate Modelling, WRF, MPI-ESM, ERA-Interim, Iberian Peninsula

---

*Email address:* [m.martalmeida@ua.pt](mailto:m.martalmeida@ua.pt) (Martinho Marta-Almeida )

## 27 1. Introduction

28 Global Climate Models (GCM) have been in use for more than a decade to study the impact  
29 of anthropogenic emission scenarios on global climate change. These models, albeit useful to un-  
30 derstand global trends and climate change behaviour, lack the spatial resolution to solve meso to  
31 local scale phenomena. Therefore, in order to assess the impact of climate change at local scales in  
32 activities of interest such as agriculture, forestry and energy production, regional climate change  
33 modelling is needed. Various techniques have been developed to downscale GCM scenarios ([Hewit-  
34 son and Crane, 1996](#); [Lo et al., 2008](#); [Racherla et al., 2012](#)). A review of the different downscaling  
35 methods can be found in [Wilby and Wigley \(1997\)](#) and [Giorgi et al. \(2004\)](#), as well in the Inter-  
36 governmental Panel on Climate Change (IPCC) Third ([Giorgi et al., 2001](#); [Mearns et al., 2001](#))  
37 and Fourth ([Christensen et al., 2007](#)) Assessment Reports. The dynamical downscaling approach  
38 relies on coarse-resolution large-scale fields from either GCMs or global reanalysis, which are used  
39 to provide the initial and boundary conditions to a nested Regional Climate Model (RCM). The  
40 pioneer European project PRUDENCE followed by ENSEMBLES ([Van der Linden and Mitchell,  
41 2009](#)) provided multi-model ensembles of RCM simulations for Europe which has been extensively  
42 analysed not only by the official modelling groups but also by the word scientific community. When  
43 constrained by a large-scale model, the RCM does not change the large-scale circulation of the  
44 GCM, while adding regional detail in response to the large scale forcing, simulating more realis-  
45 tically surface winds and temperatures over complex terrain and coastlines, as well as mesoscale  
46 processes and its variability ([Giorgi, 2006](#); [Lo et al., 2008](#)). The result is typically a highly detailed  
47 and accurate model solution over the region of interest.

48 Such implementations have been broadly used and the value added with the downscaling tech-  
49 nique has been often debated. [Castro et al. \(2005\)](#) and [Rockel et al. \(2008\)](#) have shown that the  
50 RCM can not add skill to simulations of large-scale weather features beyond what is already in  
51 the parent global model or reanalysis, since the RCM is strongly influenced by the parent model.  
52 Moreover, [Castro et al. \(2005\)](#) classified the dynamical downscaling into (1) numerical weather  
53 prediction, in which the memory of the initial conditions are not lost due to the short-term model  
54 integration; (2) regional climate simulations driven by global reanalysis, in which memory is lost,

55 but the periodically enforced lateral boundary conditions contain atmospheric observations; (3)  
56 GCMs, in which the real-world influence comes indirectly via the observed ocean boundary condi-  
57 tions driving the GCM; and (4) GCMs real-world constraints are completely absent. Considering  
58 this, the authors observed that model skill worsens as the parent global input goes from a re-  
59 analysis to a global prediction model (in which all aspects of the climate system are predicted),  
60 with intermediate steps where only some aspects of the system are prescribed (e.g., sea surface  
61 temperature).

62 In the past decade, the most common approach in regional climate simulations was to have a  
63 single initialization of large-scale fields and frequent updates of lateral boundary conditions. This  
64 approach has been shown to have several drawbacks, namely the development of flow within the  
65 RCM domain inconsistent with the driving boundary conditions. Furthermore, the internal solu-  
66 tion generated by RCMs may vary with the size of the simulation domain, as well as location and  
67 season (Miguez-Macho et al., 2004; Castro et al., 2005). To overcome this issue, the use of nudg-  
68 ing or relaxation of large-scale atmospheric circulations within the interior of the computational  
69 domain of the RCM has been applied and proven to produce successful results (Miguez-Macho  
70 et al., 2004; Bowden et al., 2012; Spero et al., 2014). This method prevents the RCM solution to  
71 drift away from the large-scale driving fields. In addition, Spero et al. (2014) has shown that the  
72 spectral nudging method was successful in keeping the simulated states close to the driving state  
73 at large scales, while generating small-scale features and thus improving model skill.

74 The implementation of a dynamical downscaling technique using a single initialization and  
75 spectral nudging to the large-scale patterns allows to perform a single spin-up while obtaining a  
76 structured and consistent solution of the regional scale climate, coping with the the soil moisture  
77 initialization as shown by Khodayar et al. (2014), while maintaining consistency between the  
78 large-scale fields of the forcing GCM (Spero et al., 2014).

79 The objective this work is to compare the results obtained with a regional scale modelling  
80 configuration for the Iberian Peninsula, forced with a GCM and forced with a global reanalysis.  
81 This validation will give us confidence of the usage of the GCM to force the regional model  
82 in forecast simulations of the future climate under predefined anthropogenic emission scenarios.

83 The manuscript provides a description of the downscaling parametrizations and a comparison of  
84 model results with observations in terms of precipitation and mean and extreme values of surface  
85 temperature.

## 86 **2. Methods**

### 87 *2.1. Regional Model*

88 The community model WRF version 3.5 (Skamarock et al., 2005) with the modifications per-  
89 formed by Fita et al. (2010) for regional climate simulation has been broadly used to produce  
90 climatological downscaling (Gula and Peltier, 2012; Bowden et al., 2012; Pinto et al., 2014) and  
91 was applied in this work to produce a dynamical climate downscaling for the Iberian Peninsula.  
92 Two sets of atmospheric global simulation results, from different sources, were used to provide  
93 initial and boundary conditions to the regional configuration. Firstly the MPI-ESM (LR) model  
94 with the r1i1p1 initialization, with 1.9° horizontal resolution and 47 hybrid sigma-pressure levels  
95 (Giorgetta et al., 2013) was used. This model participated in the Coupled Model Intercompari-  
96 son Project Phase 5 (CMIP5). As a representation of the recent-past climate, the last 20 years  
97 (1986-2005) Secondly the ERA-Interim reanalysis (Dee et al., 2011). The model used to generate  
98 the reanalysis uses a 4D-variational analysis on a spectral grid with triangular truncation of 255  
99 waves T255 with 80km (N128) - reduced points - Gaussian grid and a hybrid coordinate system  
100 with 60 vertical levels.

101 These two configurations are named WRF-MPI (WRF driven by MPI-ESM) and WRF-ERA  
102 (WRF driven by ERA-Interim) hereinafter.

103 The WRF lateral boundary conditions were provided to the model at six hour intervals, in-  
104 cluding the sea surface temperature update, and a spectral nudging for wave length larger than  
105 1000 km was considered (Miguez-Macho et al., 2004). Ferreira (2007) has tested several model  
106 parametrizations configuration for the Iberian Peninsula using the WRF model, comparing the  
107 model outputs against observations. Considering his findings, the set of parametrizations used in  
108 the model physical configuration were: WRF Single-moment 6-class Microphysical Scheme (Hong  
109 et al., 2006); Dudhia Shortwave radiation scheme (Dudhia, 1989); RRTMG (Rapid Radiative

110 Transfer Model) longwave radiation model (Mlawer et al., 1997); MM5 similarity surface layer  
111 scheme (Zhang and Anthes, 1982); Noah Land Surface Model (Tewari et al., 2004); Yonsei Univer-  
112 sity Planetary Boundary Layer scheme (Hong and Lim, 2006) and Grell-Freitas Ensemble Scheme  
113 for cumulus parametrization (Grell and Freitas, 2013).

114 A similar set of parameterisations are used by the Group of Meteorology and Climatology from  
115 Aveiro University (<http://climetua.ua.pt>) to perform analysis and forecasts for the Portuguese  
116 region. Data produced by the group has been successfully used for weather forecasting and to  
117 force a biogeochemical ocean model for the Portuguese and Galician waters (Marta-Almeida et al.,  
118 2012).

119 Due to the importance of land use accuracy, the Coordination of Information on the En-  
120 vironment Land Cover (CORINE, Bossard et al. (2000)) was implemented recategorized to be  
121 recognizable by the WRF model. This conversion of CORINE data into WRF categories followed  
122 Pineda et al. (2004). Teixeira et al. (2014) performed sensitivity test for the usage of this dataset  
123 in WRF simulations obtaining positive results.

124 The regional WRF implementation uses three domains online nested with increasing resolution  
125 at a downscaling ratio of 3. The domains are illustrated in Figure 1. The coarser domain, D-1,  
126 covers part of the North Atlantic ocean and most of Europe, using a horizontal resolution of 81  
127 km. The smallest domain, with 9 km resolution, solves the Iberian Peninsula extending off-coast  
128 several hundreds of km.

## 129 *2.2. Model validation*

130 Observational data for model validation was obtained for Spain and Portugal independently.  
131 The Spanish dataset (Spain02, Herrera et al. (2012, 2014-submitted)), developed by the University  
132 of Cantabria, includes long term (from 1971 to end of 2010) gridded daily precipitation and near  
133 surface temperature (daily maximum, minimum and mean) at  $0.11^\circ$  resolution. The Portuguese  
134 dataset, created by the Portuguese Institute of Meteorology, includes only precipitation and at a  
135 lower horizontal resolution ( $0.2^\circ$ ), but it is still the best observational product available. It includes  
136 data from 1950 to the end of 2013 (Belo-Pereira et al., 2011).

137 From these datasets of temperature and precipitation it was created a daily climatology. Then  
138 a temporal K-Means cluster analysis (MacQueen, 1967) was performed on the seasonal subsets  
139 resulting in a spatial subdivision of the domain in regions with similar temporal behaviour (mag-  
140 nitude and variability). The model results, from the higher resolution domain D-3, were then  
141 compared with observations using the clusters as a natural division of the domain. Daily clima-  
142 tologies of modelled precipitation and, maximum, minimum and mean temperature were created  
143 to compare with the daily climatologies of the observed data. Finally, the probability distribu-  
144 tions of the model output variables inside each cluster and for each season were compared with  
145 the corresponding probability distributions of the observations. The data inside each cluster was,  
146 thus, spatially averaged and the mean of the resulting time series was removed. The result was a  
147 centred probability distributions of precipitation and temperature, in distinct regions of Portugal  
148 and Spain, for the four seasons. The aim was to access if the shape of the observational distribu-  
149 tions could be reproduced by the model forced by both a GCM and a reanalysis. If WRF-MPI and  
150 WRF-ERA probability distributions present similar differences to the observational distributions,  
151 we have the confidence to use the GCM MPI-ESM (LR) to drive WRF for climatic simulations of  
152 future scenarios.

153 The K-Means cluster analysis is a non-hierarchical clustering method which starts by computing  
154 the centroids for each cluster and then calculates the distances between the current data vector  
155 and each of the centroids, assigning the vector to the cluster whose centroid is closest to it. Since  
156 this is a dynamic method, meaning that vectors can change cluster after being assigned to it, this  
157 process is repeated until all vectors are assigned a cluster and their members are closest to the  
158 centroid than to the mean of other clusters (Wilks, 2011). The determination of the number of  
159 clusters was done using the Caliński and Harabasz (1974) pseudo F-statistic, which is based on the  
160 maximization of the ratio of between-cluster variance to within-cluster variance. This approach of  
161 domain decomposition has been successfully applied for European temperature and precipitation  
162 by Carvalho et al. (2015), and for Iberian Peninsula precipitation by Parracho et al. (2015). This  
163 clustering regionalisation technique is a robust method and with physical significance, since it  
164 gathers points with comparable variability. Arbitrary methods of domain partitioning, like the

165 usage of political boundaries or a fixed number of empirical regions based on distance to coast or  
166 other frontiers, for instance, lacks physical meaning, although still being commonly employed in  
167 climate and modeling studies.

168 Our domain decomposition, using the observational datasets, identified four clusters for each  
169 season of Spanish temperatures and precipitation, and three clusters for Portuguese precipitation.

170 The probability density functions were estimated using a Gaussian Kernel Density Estimator  
171 (Rosenblatt, 1956; Parzen, 1962) with automatic bandwidth determination using the Scott's Rule  
172 (Scott, 2009). The comparison of probability distributions of the observed and modelled vari-  
173 ables was done via the Kolmogorov-Smirnov test (KS-test, Kolmogorov (1933); Smirnov (1948)).  
174 KS-test is a nonparametric test that compares the cumulative distributions of two datasets. This  
175 test is robust to outliers, just like the other commonly used Mann-Whitney test (MW-test, Mann  
176 and Whitney (1947)), but is more robust to detect changes in the shape of the distribution than  
177 the MW-test (Lehmann and D'Abbrera, 2006).

### 178 3. Results

179 The validation of WRF forced by the climate model (WRF-MPI) and by the reanalysis (WRF-  
180 ERA) is made by comparing the probability distributions of the average daily climatologies inside  
181 regions with temporal similarities (clusters). This analysis was done for each of the four seasons  
182 and for temperature and precipitation over Spain, and for precipitation over Portugal.

183 The results for the maximum near surface temperature is shown in Figure 2. The figure is  
184 organised so that each row corresponds to one season, the first column shows the clusters subdivi-  
185 sion and the other columns show the probability distributions of the observations (Ob) and model  
186 results. The KS-test statistic (d-value, maximum distance between the cumulative distributions)  
187 and p-value of the pairs Ob vs WRF-ERA and Ob vs WRF-MPI are shown inside each subplot.  
188 High p-values or low d-values indicate the null hypothesis that both groups were sampled from  
189 populations with similar distribution, cannot be rejected.

190 The results of maximum temperature identify a hotter region in southern Spain and a colder  
191 region occupying in general all the north of the Peninsula and a small region in the south (west An-

192 dalucía). The winter (DJF) and summer (JJA) results clear show a larger departure of WRF-MPI  
193 from the observations, both in terms of magnitude and shape of the distribution, with associated  
194 p-values decreasing to 0.02 and 0.05 in the summer. Spring WRF-MPI has a much better corre-  
195 spondence to the observations. In autumn we have a mixed WRF-MPI behaviour, with regions  
196 with high p-values and regions with low p-values. WRF-ERA has much higher p-value in all the  
197 regions and all seasons, as can be easily observed by the shape of the distributions which are very  
198 close to the Ob distributions.

199 The probability distributions of the mean temperature (Figure 3) show a similar spatial pat-  
200 tern of the cluster subdivisions, with a northward decrease of temperature. The KS-test exhibits  
201 in general improved values for WRF-MPI (compared to the values obtained for maximum tem-  
202 perature), especially for the summer months, showing an increase in the p-values above the 0.05  
203 threshold and a decrease in the d-values of all the cluster regions.

204 Minimum temperatures (Figure 4) show better agreement for WRF-MPI, comparable to WRF-  
205 ERA in some seasons/regions, and even higher for the colder summer regions. A much closer shape  
206 of the distributions is evident, relatively to the maximum and mean temperatures.

207 Regarding daily climatological total precipitation over Spain (Figure 5), a very well defined  
208 subdivision of the region was obtained with the cluster analysis, with Galicia and Northern Spain  
209 having higher precipitation and the central and Mediterranean regions with lower values. An  
210 overall agreement between model results and observations was obtained, considering the difficulty  
211 to model the convective precipitation (e.g. Yang et al., 2012). Still, low p-values are obtained for  
212 high precipitation regions during winter. There is not a clear definition of which model results  
213 perform better (WRF-MPI or WRF-ERA). During the summer, the lowest precipitation region  
214 shows a very high p-value for WRF-MPI (0.99) and very low for WRF-ERA (0.00). Spring and  
215 autumn show reasonably good and comparable p-values for both models. The worst season/region  
216 combination in terms of model capacity to follow observations is the winter high precipitation  
217 Galician region, where p-values are below 0.05.

218 The results for precipitation over Portugal, depicted in Figure 6, show maximum values in the  
219 North Atlantic region through all the year. Lowest precipitation is found in the southern region

220 and in general in all the eastern side. The best comparison of probability distributions occur during  
221 the autumn. In all other seasons, p-values are notoriously low. In the three regions and for the  
222 seasons winter to spring, WRF-MPI values are three times lower than 0.05 and WRF-ERA values  
223 are seven times below 0.05.

#### 224 4. Analysis

225 The regionalisation of the observational domains, followed by spatial averanging in each sub-  
226 region, decreased the dimension of the data, allowing the representation of the annual cycle of  
227 temperature and precipitation fields by probability distributions for each season, appears to be  
228 a successful technique. The subregions obtained obey the empirical and bibliographic knowledge  
229 on the intensity and variability of temperature and precipitation of the Iberian Peninsula, namely  
230 the high rain in northwest Portugal, Galicia and the rest of northern Spain, the drier southern  
231 Portugal and southern/central Spain, and the higher temperatures in southern Spain.

232 The subregions have complex geometries, and even having been calculated according to the  
233 intensity and variability of daily climatologies, we get satisfied whenever the statistical test com-  
234 paring the distribution of observed data and model result return a p-value above the threshold  
235 0.05 (the usual level of significance). Values higher than this indicate we should not reject the  
236 hypothesis that the sets belong to populations with the same probability distribution. This hap-  
237 pened in most of the regions/seasons for Spanish temperature and precipitation. The zero p-value  
238 obtained for the WRF-ERA Spanish summer precipitation in the lowest precipitation region is not  
239 significant because the days without precipitation were not removed before the analysis. So, even  
240 a small precipitation difference may result in high relative differences and hence a bad comparison  
241 with the KS-test. Low p-values are also obtained for the high precipitation region (west Galicia)  
242 during the winter. This may be associated with the difficulty of simulating convective precipitation  
243 (e.g. [Yang et al., 2012](#)), even using convective resolving resolution. Some effort could be positive  
244 on the attempt to improve the capacity of the model to reproduce the highest precipitation value,  
245 namely by assessing the model performance with different combinations of horizontal and vertical  
246 resolution and convective parameterisations.

247 The highest temperatures returned by the model forced by the CGM (WRF-MPI) also show  
248 poor comparison with observations. On the other hand, the model forced by reanalysis compares  
249 very well. Reanalysis is based on the usage of realistic initial conditions and continuous assimila-  
250 tions. So, in the end, the result obtained for the very difficult to reproduce maximum temperature  
251 (e.g. [Sillmann et al., 2014](#)), is not strange. We accept the result specially because the probability  
252 distributions of WRF-MPI actually exhibit, with distortions, the same features of the observations.

253 The results for the Portuguese precipitation are quite surprising. Over Spain, the comparison  
254 among the datasets is fairly good, but over Portugal the distributions differ substantially, even  
255 without important geographic differences that could justify such behaviour. Basically the unique  
256 distinction is the source of the datasets. The Portuguese dataset has about half the resolution  
257 of the Spanish dataset and was created based on Ordinary Kriging Interpolation, and a sparse  
258 observational network in large portions of the country. The Spanish higher resolution dataset  
259 is continuously evolving and includes improved interpolation methodologies and data correction  
260 schemes.

## 261 5. Conclusion

262 The atmospheric model WRF was parameterised to perform high resolution climate simulations  
263 of a nested configuration of the Iberian Peninsula. In order to validate the model ability to simulate  
264 scenarios for the future, driven by a GCM, we decided to do two simulations for the past (20 years,  
265 1996 to 2005), one forced by the GCM, other forced by ERA-Interim. The chosen GCM was  
266 MPI-ESM (LR). If historic simulations with both forcings result in a similar comparison with  
267 observations, we shall feel justified the continuity of the usage of the GCM to force future climate  
268 simulations of WRF.

269 The observational datasets used include extremes and mean temperature over Spain and precip-  
270 itations for both Portugal and Spain. The comparison was done in terms of probability distribution  
271 of daily climatologies inside subregions of the observational domain. These subregions were cal-  
272 culated using a cluster analysis technique, which gathers spatially points with similar temporal  
273 behaviour. Inside each cluster, observed and modelled data was spatially averaged and the prob-

274 ability distribution of the resulting time series was estimated. This procedure was done for each  
275 season separately.

276 The results show an overall acceptable comparison of both models with observations, with sea-  
277 sons/regions where model forced with reanalysis (WRF-ERA) performs better, but also occasions  
278 when the comparison for WRF-MPI was better. In general, however, WRF-ERA gave probability  
279 distributions closer to the observed ones.

280 In spite of the difficulty of simulate extremes of atmospheric variables, like maximum tem-  
281 perature and extreme precipitation, in continuous long term simulations, without reinitialisation  
282 and/or data assimilation, the statistical test used to compare the probability distributions gave in  
283 general good results, i.e., in most of the occasions it cannot be rejected that the datasets compared  
284 belong to the same distribution.

285 The worst results were obtained for the precipitation over Portugal, in disagreement with the  
286 comparison done for precipitation over Spain. Since apparently more effort has been dedicated to  
287 the Spanish dataset, we are forced to trust our comparison with the Spanish precipitation. Also,  
288 even assuming the same quality of the observations, the differences in the observational network,  
289 differences in the resolution of the final dataset, in the data correction approaches and interpo-  
290 lations methodologies employed, may result in important discrepancies among the observational  
291 datasets.

292 Considering the results obtained, we feel confidence on the usage of the WRF-MPI to perform  
293 climate simulations of the future. Such task is already underway and the results will be analysed  
294 soon.

## 295 **Acknowledgements**

296 This study was supported by FEDER funds through the Programa Operacional Factores de  
297 Competitividade COMPETE and by Portuguese national funds through FCT - Fundação para  
298 a Ciência e a Tecnologia, within the framework of the following projects: CLIPE Project Ref-  
299 erence PTDC/AAC-CLI/111733/2009; CLICURB EXCL/AAG-MAA/0383/2012. The authors  
300 thank AEMET and UC for the data provided for this work (Spain02 dataset, <http://www.>

301 [meteo.unican.es/datasets/spain02](http://meteo.unican.es/datasets/spain02)) The authors thank IPMA for the Portuguese precipita-  
302 tion dataset.

## 303 6. References

304 Belo-Pereira, M., Dutra, E., Viterbo, P., 2011. Evaluation of global precipitation data sets over  
305 the Iberian Peninsula. *Journal of Geophysical Research* 116.

306 Bossard, M., Feranec, J., Otahel, J., 2000. CORINE land cover technical guide - Addendum 2000.  
307 Tech. Rep. 40, European Environmental Agency, Copenhagen.

308 Bowden, J. H., Otte, T. L., Nolte, C. G., Otte, M. J., 2012. Examining interior grid nudging  
309 techniques using two-way nesting in the WRF model for regional climate modeling. *Journal of*  
310 *Climate* 25, 2805–2823.

311 Caliński, T., Harabasz, J., 1974. A dendrite method for cluster analysis. *Communications in*  
312 *Statistics-theory and Methods* 3, 1–27.

313 Carvalho, M. J., Melo-Gonçalves, P., Teixeira, J. C., Rocha, A. M., 2015. Regionalization of Europe  
314 based on a K-Means Cluster Analysis of the climate change of Temperatures and Precipitation.  
315 *Physics and Chemistry of the Earth* (current issue).

316 Castro, C. L., Pielke, R. A., Leoncini, G., 2005. Dynamical downscaling: Assessment of value  
317 retained and added using the Regional Atmospheric Modeling System (RAMS). *Journal of Geo-*  
318 *physical Research: Atmospheres* 110.

319 Christensen, J., Hewitson, B., Busuioc, A., Chen, A., Gao, X., Held, I., Jones, R., Kolli, R., Kwon,  
320 W.-T., Laprise, R., na Rueda, V. M., Mearns, L., Menéndez, C., Räisänen, J., Rinke, A., Sarr,  
321 A., Whetton, P., 2007. *Regional climate projectios*. Cambridge University Press.

322 Dee, D., Uppala, S., Simmons, A., Berrisford, P., Poli, P., Kobayashi, S., Andrae, U., Balmaseda,  
323 M., Balsamo, G., Bauer, P., et al., 2011. The ERA-Interim reanalysis: Configuration and per-

324 performance of the data assimilation system. Quarterly Journal of the Royal Meteorological Society  
325 137, 553–597.

326 Dudhia, J., 1989. Numerical study of convection observed during the winter monsoon experiment  
327 using a mesoscale two-dimensional model. Journal of the Atmospheric Sciences 46, 3077–3107.

328 Ferreira, A., 2007. Sensibilidade às parametrizações físicas do WRF nas previsões à superfície em  
329 Portugal Continental. Relatório de estágio em meteorologia e oceanografia Física. Universidade  
330 de Aveiro.

331 Fita, L., Fernández, J., Garcia-Diez, M., 2010. CLWRF: WRF modifications for regional climate  
332 simulation under future scenarios. In: 11<sup>th</sup> WRF Users’s Workshop. NCAR Boulder CO.

333 Giorgetta, M. A., Jungclaus, J., Reick, C. H., Legutke, S., Bader, J., Böttinger, M., Brovkin, V.,  
334 Crueger, T., Esch, M., Fieg, K., et al., 2013. Climate and carbon cycle changes from 1850 to  
335 2100 in MPI-ESM simulations for the Coupled Model Intercomparison Project phase 5. Journal  
336 of Advances in Modeling Earth Systems 5, 572–597.

337 Giorgi, F., dec 2006. Regional climate modeling: Status and perspectives. Journal de Physique IV  
338 France 139, 101–118.

339 Giorgi, F., Bi, X., Pal, J., 2004. Mean, interannual variability and trends in a regional climate  
340 change experiment over Europe. I. Present-day climate (1961–1990). Climate Dynamics 22,  
341 733–756.

342 Giorgi, F., Jones, R., P, W., H, V. S., Fu, G., Mearns, L. O., Hewitson, B., Christensen, H., Hulme,  
343 M., 2001. Regional climate information evaluation and projections. Cambridge University Press,  
344 Cambridge, pp. 583–638.

345 Grell, G. A., Freitas, S. R., 2013. A scale and aerosol aware stochastic convective parameterization  
346 for weather and air quality modeling. Atmospheric Chemistry and Physics 13, 845–23.

347 Gula, J., Peltier, W. R., 2012. Dynamical downscaling over the Great Lakes basin of North America  
348 using the WRF regional climate model: The impact of the Great Lakes system on regional  
349 greenhouse warming. *Journal of Climate* 25, 7723–7742.

350 Herrera, S., Gutiérrez, J. M., Ancell, R., Pons, M., Frías, M., Fernández, J., 2012. Development and  
351 analysis of a 50-year high-resolution daily gridded precipitation dataset over Spain (Spain02).  
352 *International Journal of Climatology* 32, 74–85.

353 Herrera, S., et al., 2014-submitted. Update of the Spain02 gridded observational dataset for Euro-  
354 CORDEX evaluation: Assessing the effect of the interpolation methodology. *International Jour-  
355 nal of Climatology*.

356 Hewitson, B., Crane, R., 1996. Climate downscaling: techniques and application. *Climate Research*  
357 7, 85–95.

358 Hong, S.-Y., Lim, J.-O. J., 2006. The WRF single-moment 6-class microphysics scheme (WSM6).  
359 *Asia-Pacific Journal of Atmospheric Sciences* 42, 129–151.

360 Hong, S.-Y., Noh, Y., Dudhia, J., 2006. A new vertical diffusion package with an explicit treatment  
361 of entrainment processes. *Monthly Weather Review* 134 (9), 2318–2341.

362 Khodayar, S., Sehlinger, A., Feldmann, H., Kottmeier, C., 2014. Sensitivity of soil moisture ini-  
363 tialization for decadal predictions under different regional climatic conditions in Europe. *Inter-  
364 national Journal of Climatology*.

365 Kolmogorov, A. N., 1933. Sulla determinazione empirica di una legge di distribuzione. *Giornale*  
366 *dell Istituto Italiano degli Attuari* 4, 83–91.

367 Lehmann, E. L., D’Abrera, H. J., 2006. *Nonparametrics: statistical methods based on ranks*.  
368 Springer New York.

369 Lo, J. C.-F., Yang, Z.-L., Pielke, R. A., 2008. Assessment of three dynamical climate downscaling  
370 methods using the Weather Research and Forecasting (WRF) model. *Journal of Geophysical*  
371 *Research: Atmospheres* 113.

- 372 MacQueen, J. B., 1967. Some methods for classification and analysis of multivariate observations.  
373 In: 5<sup>th</sup> Berkeley Symposium on Mathematical Statistics and Probability. University of California  
374 Press, University of California Press, Berkeley, pp. 281–297.
- 375 Mann, H. B., Whitney, D. R., mar 1947. On a test of whether one of two random variables is  
376 stochastically larger than the other. *The Annals of Mathematical Statistics* 18, 50–60.
- 377 Marta-Almeida, M., Reboreda, R., Rocha, C., Dubert, J., Nolasco, R., Cordeiro, N., Luna, T.,  
378 Rocha, A., e Silva, J. D. L., Queiroga, H., Peliz, A., Ruiz-Villarreal, M., may 2012. Towards  
379 Operational Modeling and Forecasting of the Iberian Shelves Ecosystem. *PLoS ONE* 7, e37343.
- 380 Mearns, L. O., Hulme, M., Carter, T. R., P, W., 2001. Climate scenario development. Cambridge  
381 University Press, Cambridge, pp. 739–768.
- 382 Miguez-Macho, G., Stenchikov, G. L., Robock, A., 2004. Spectral nudging to eliminate the effects  
383 of domain position and geometry in regional climate model simulations. *Journal of Geophysical*  
384 *Research: Atmospheres* 109.
- 385 Mlawer, E. J., Taubman, S. J., Brown, P. D., Iacono, M. J., Clough, S. A., 1997. Radiative trans-  
386 fer for inhomogeneous atmospheres: RRTM, a validated correlated-k model for the longwave.  
387 *Journal of Geophysical Research: Atmospheres* 102, 16663–16682.
- 388 Parracho, A. C., Melo-Gonçalves, P., Rocha, A. M., 2015. Regionalization of precipitation for the  
389 Iberian Peninsula. *Physics and Chemistry of the Earth (current issue)*.
- 390 Parzen, E., sep 1962. On estimation of a probability density function and mode. *The Annals of*  
391 *Mathematical Statistics* 33, 1065–1076.
- 392 Pineda, N., Jorba, O., Jorge, J., Baldasano, J., 2004. Using NOAA AVHRR and SPOT VGT data  
393 to estimate surface parameters: application to a mesoscale meteorological model. *International*  
394 *Journal of Remote Sensing* 25, 129–143.

395 Pinto, J. O., Monaghan, A. J., Delle Monache, L., Vanvyve, E., Rife, D. L., 2014. Regional  
396 assessment of sampling techniques for more efficient dynamical climate downscaling. *Journal of*  
397 *Climate* 27, 1524–1538.

398 Racherla, P. N., Shindell, D. T., Faluvegi, G. S., 2012. The added value to global model projections  
399 of climate change by dynamical downscaling: A case study over the continental US using the  
400 GISS-ModelE2 and WRF models. *Journal of Geophysical Research: Atmospheres* 117.

401 Rockel, B., Castro, C. L., Pielke, R. A., von Storch, H., Leoncini, G., 2008. Dynamical downscaling:  
402 Assessment of model system dependent retained and added variability for two different regional  
403 climate models. *Journal of Geophysical Research: Atmospheres* 113.

404 Rosenblatt, M., sep 1956. Remarks on some nonparametric estimates of a density function. *The*  
405 *Annals of Mathematical Statistics* 27, 832–837.

406 Scott, D. W., 2009. *Multivariate density estimation: theory, practice, and visualization*. Vol. 383.  
407 John Wiley & Sons.

408 Sillmann, J., Donat, M. G., Fyfe, J. C., Zwiers, F. W., 2014. Observed and simulated temperature  
409 extremes during the recent warming hiatus. *Environmental Research Letters* 9, 064023.

410 Skamarock, W. C., Klemp, J. B., Dudhia, J., Gill, D. O., Barker, D. M., Wang, W., Powers, J. G.,  
411 2005. A description of the advanced research WRF version 2. Tech. rep., DTIC Document.

412 Smirnov, N., 1948. Table for estimating the goodness of fit of empirical distributions. *The Annals*  
413 *of Mathematical Statistics* 19, 279–281.

414 Spero, T. L., Otte, M. J., Bowden, J. H., Nolte, C. G., 2014. Improving the representation of clouds,  
415 radiation, and precipitation using spectral nudging in the Weather Research and Forecasting  
416 model. *Journal of Geophysical Research: Atmospheres* 119, 11–682.

417 Teixeira, J., Carvalho, A., Carvalho, M., Luna, T., Rocha, A., 2014. Sensitivity of the WRF model  
418 to the lower boundary in an extreme precipitation event—Madeira island case study. *Natural*  
419 *Hazards and Earth System Science* 14, 2009–2025.

- 420 Tewari, M., Chen, F., Wang, W., Dudhia, J., LeMone, M., Mitchell, K., Ek, M., Gayno, G.,  
421 Wegiel, J., Cuenca, R., 2004. Implementation and verification of the unified NOAH land surface  
422 model in the WRF model. 20<sup>th</sup> conference on weather analysis and forecasting/16<sup>th</sup> conference  
423 on numerical weather prediction, pp. 11–15.
- 424 Van der Linden, P., Mitchell, JFB, e., 2009. ENSEMBLES: Climate Change and its Impacts:  
425 Summary of research and results from the ENSEMBLES project. Met Office Hadley Centre,  
426 FitzRoy Road, Exeter EX1 3PB, UK 160.
- 427 Wilby, R. L., Wigley, T., 1997. Downscaling general circulation model output: a review of methods  
428 and limitations. *Progress in Physical Geography* 21, 530–548.
- 429 Wilks, D. S., 2011. *Statistical methods in the atmospheric sciences*. Vol. 100. Academic press.
- 430 Yang, B., Qian, Y., Lin, G., Leung, R., Zhang, Y., 2012. Some issues in uncertainty quantification  
431 and parameter tuning: a case study of convective parameterization scheme in the WRF regional  
432 climate model. *Atmospheric Chemistry and Physics* 12, 2409–2427.
- 433 Zhang, D., Anthes, R. A., 1982. A high-resolution model of the planetary boundary layer-sensitivity  
434 tests and comparisons with SESAME-79 data. *Journal of Applied Meteorology* 21, 1594–1609.

435 **7. List of Figures**

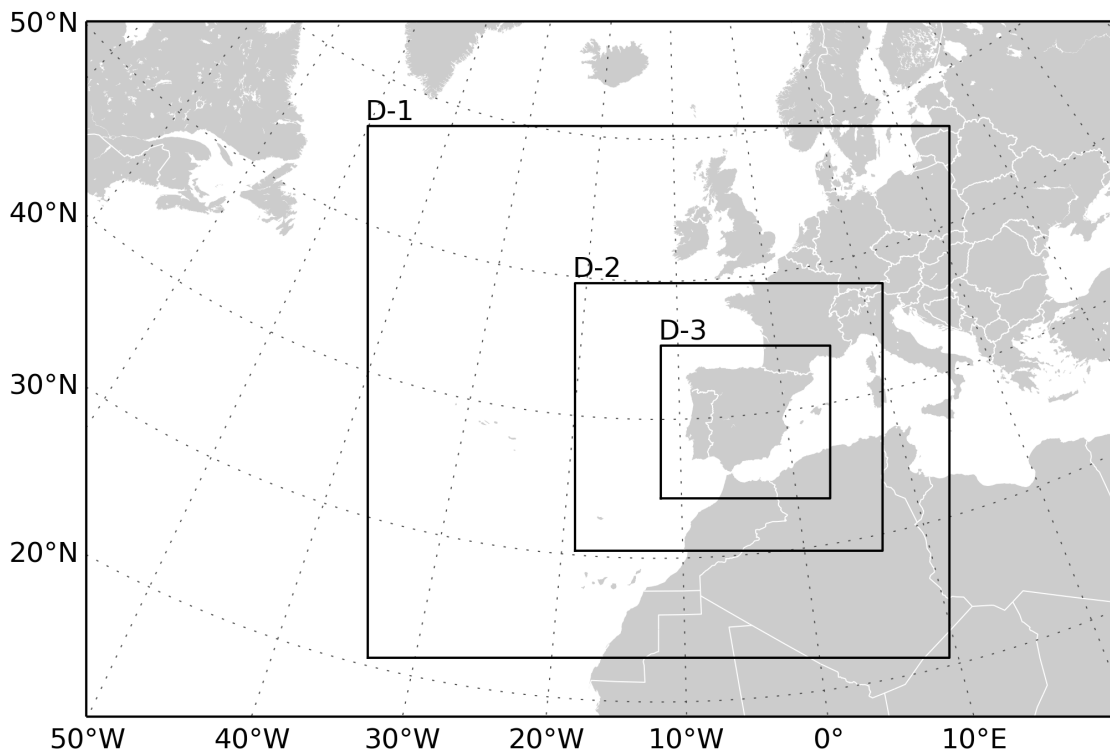


Figure 1: Model domain used in the regional WRF implementation. Model ran in 2-way nesting mode with increasing domain resolutions of 81, 27 and 9 km.

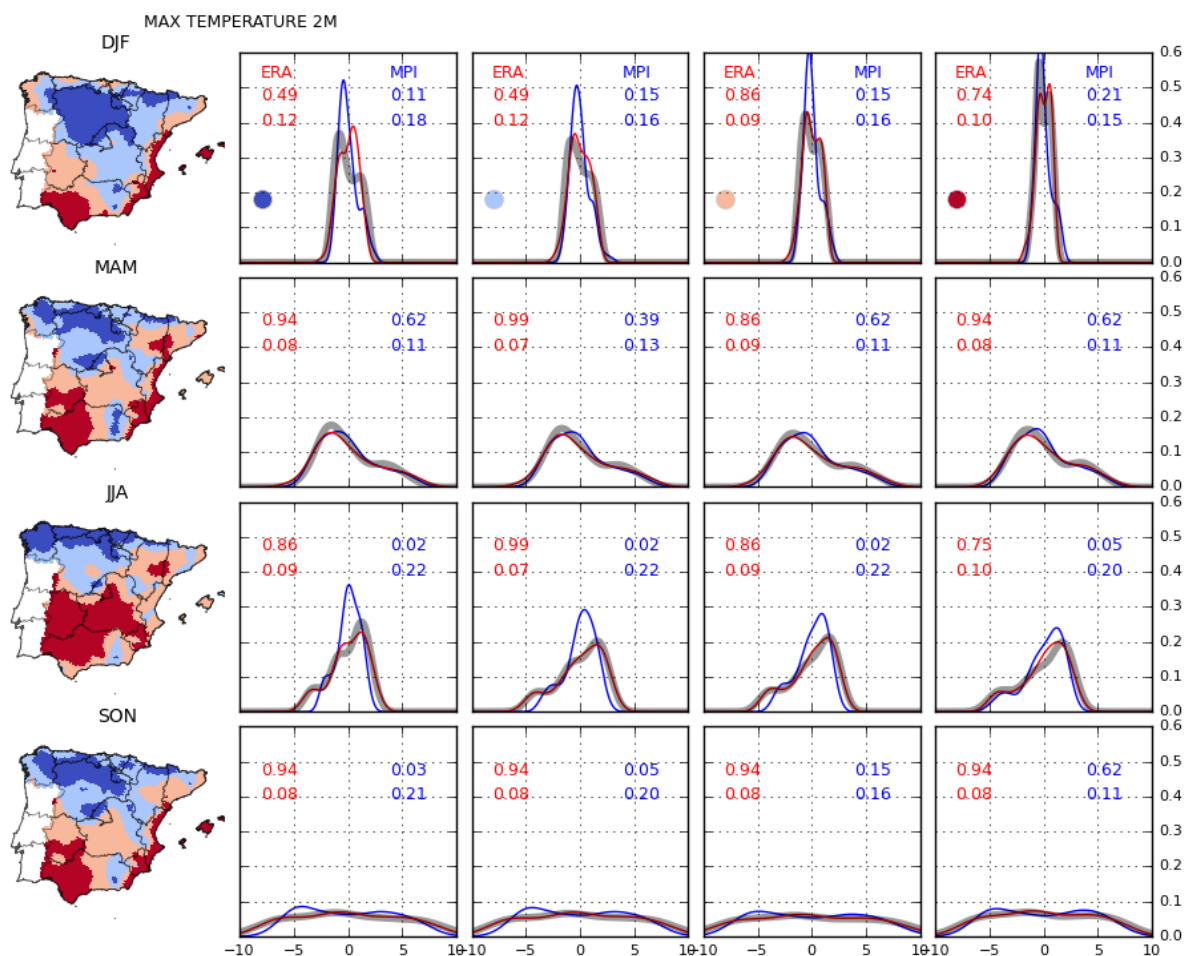


Figure 2: Regionalisation of the observed Spanish maximum temperature ( $^{\circ}\text{C}$ ) daily climatology and comparison of observed and modelled probability distribution of the spatial average inside each subregion. The probability distribution of the observations corresponds to the grey line; red line corresponds to the model forced by the ERA-Interim reanalysis (WRF-ERA); blue line corresponds to WRF model results forced with the MPI GCM (WRF-MPI). The numbers inside the subplots indicate the KS-test statistic (down) and p-value (up) corresponding to the comparison of observations with WRF-ERA (red) and with WRF-MPI (blue). Each row refers to one season (DJF means December, January and February, etc). The subplots are ordered with increasing mean value of the observed variable (subtracted from the data prior to the estimation of the probability distributions), and the corresponding cluster is indicated by the colour of the circular marker inside the winter subplots ( $1^{\text{st}}$  row).

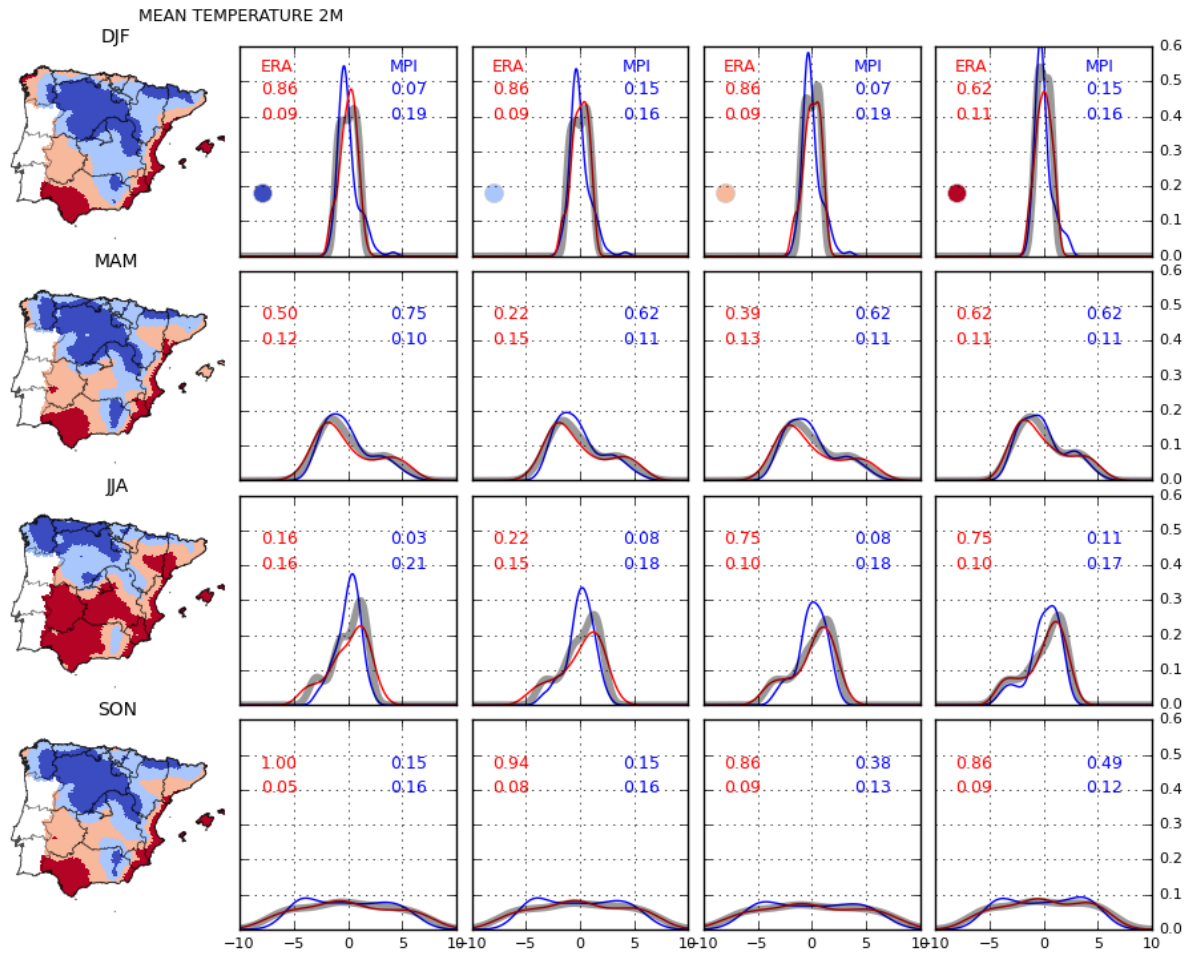


Figure 3: Same as Figure 2 but for mean temperature.

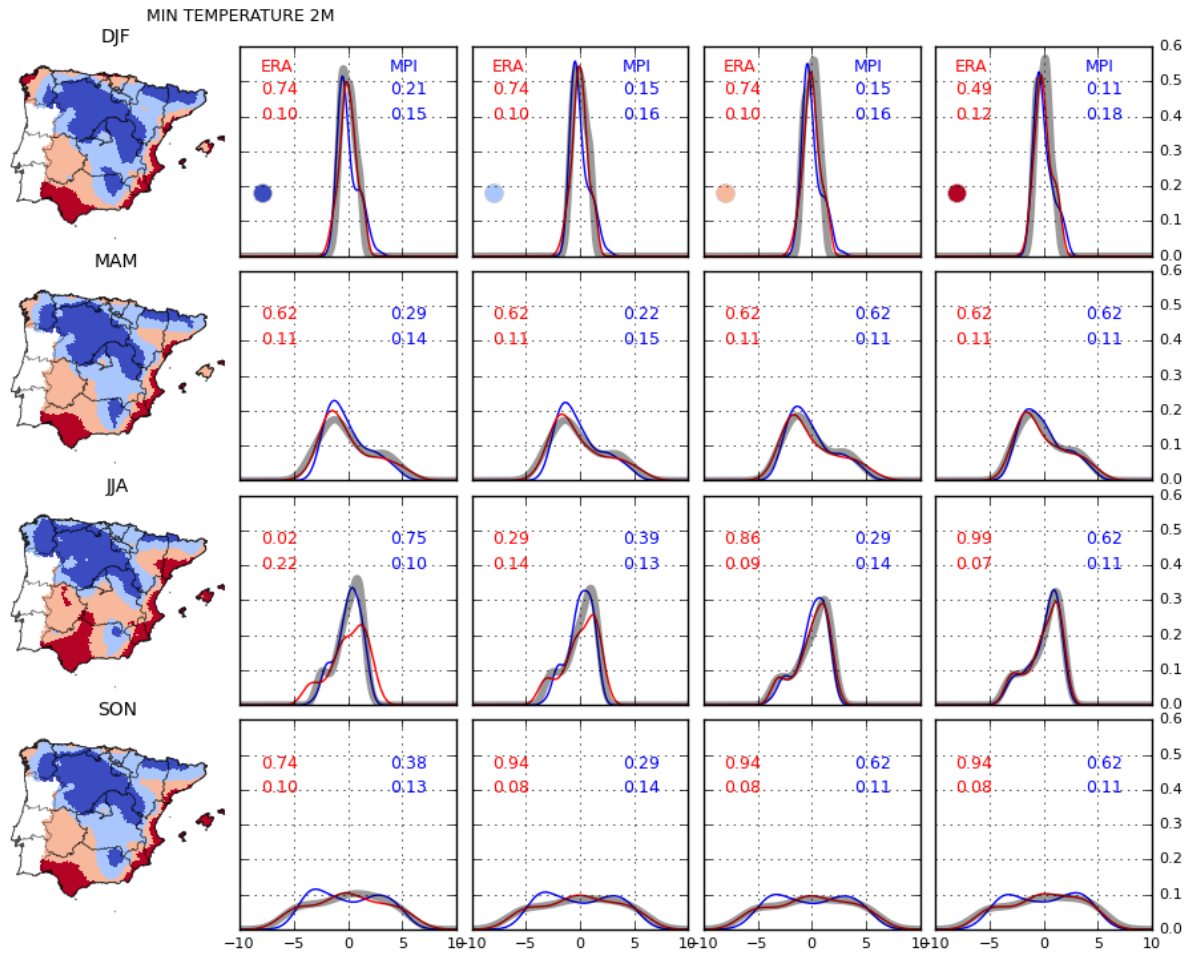


Figure 4: Same as Figure 2 but for minimum temperature.

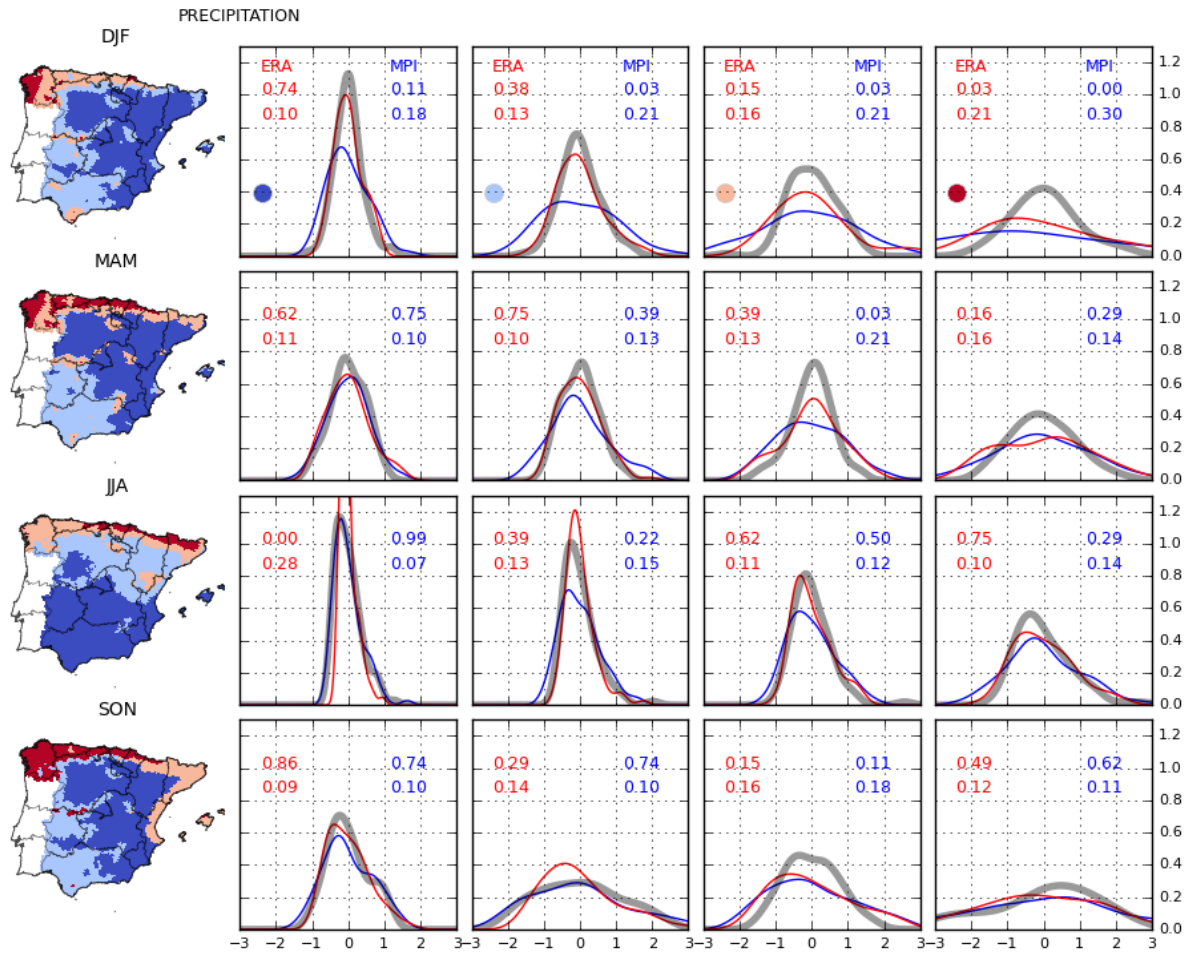


Figure 5: Same as Figure 2 but for total precipitation ( $\text{mm day}^{-1}$ ).

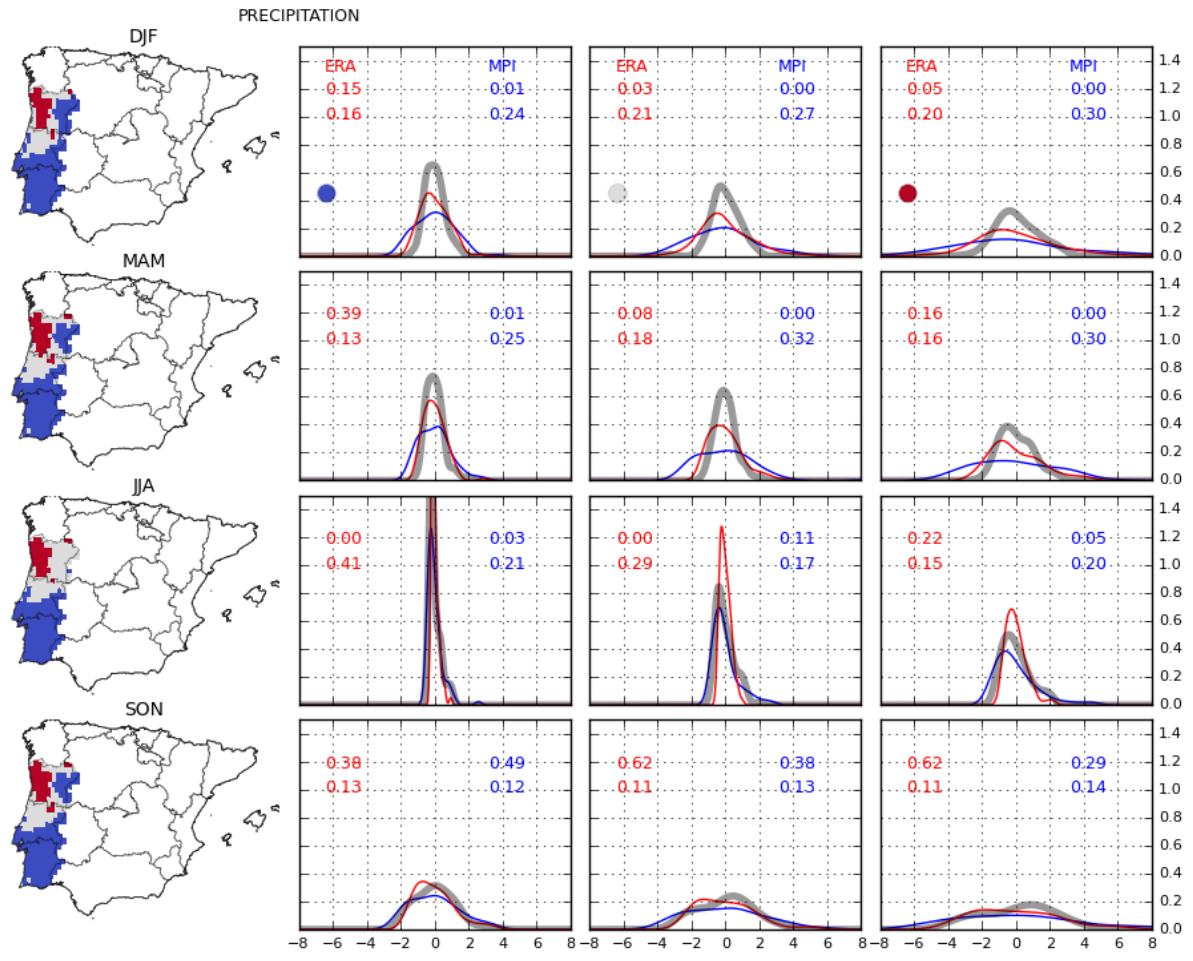


Figure 6: Same as Figure 5 but for the total precipitation ( $\text{mm day}^{-1}$ ) over Portugal.